Operating and Ambient Condition Influences on Aircraft Gas Turbine NO_x Emissions

W. S. Blazowski,* D. E. Walsh,† and K. D. Mach‡
Air Force Aero Propulsion Laboratory, Wright-Patterson Air Force Base, Ohio

This paper deals with a simplified NO_x emission model which analyzes the effects of humidity and primary zone flame temperature on the NO formation processes. Ambient temperature and humidity corrections are proposed. Methods of predicting stratospheric NO_x emissions and of correcting reduced-pressure combustor rig data to full pressure conditions are also proposed. Emission levels and trends of future combustors designed to minimize NO_x are examined.

I. Introduction

IN July of 1973, the United States Environmental Protection Agency published standards to limit emissions of carbon monoxide, total hydrocarbons, smoke, and oxides of nitrogen from aircraft engines.[1] This paper is concerned with the emission of oxides of nitrogen ,NO and NO_2, from nonafterburning aircraft turbine engines. These emissions are collectively expressed as NO_x.

Ground level emission of NO_x by aircraft is of concern principally because of NO_2 participation in atmospheric photochemical reactions which result in smog. Additional possible problems with respect to stratospheric NO emissions have been identified. It has been suggested that supersonic transport aircraft may inject sufficient NO into the stratosphere to alter the present concentration of ozone at these altitudes. Such an event would affect the average levels of ultraviolet light incident on the earth's surface and result in possible environmental damage.

NO_x emission data have been obtained for many types of non-afterburning aircraft turbine engines using techniques as described in Aerospace Recommended Practice 1256.[2] In certain cases, such as altitude data acquisition, departures from the prescribed method are necessary. Available data indicate that NO_x emissions are sensitive to ambient temperature and humidity. The July EPA standards recognized this problem and have confirmed the future requirement for ambient temperature and humidity correction factors. Future reporting of emission measurement will require documentation of ambient conditions as well as final corrected engine emission parameters. Humidity and ambient temperature correction factors are proposed in this paper.

To derive these correction factors, a relatively simple model for NO_x prediction was developed. Comparison of the model's results with available data is quite satisfactory and thereby lends confidence to its overall validity. However, the model's main utility is not to predict absolute NO_x emission levels but rather to assess emission trends caused by variations in operating and ambient conditions.

In addition to accounting for ambient temperature and humidity, the model has broader applications including: 1) correction of data to different Mach numbers and/or altitude conditions; 2) determination of the effect of typical altitude test cell humidities on NO_x emission; 3) correction of data obtained at reduced pressures in a combustor rig to full (or design) pressure; and 4) prediction of the ideal effect of water injection to reduce NO_x. These subjects are addressed in the following sections. Recognizing that future low-NO_x-emission combustors with low primary zone equivalence ratios will have different NO_x emission characteristics, important results have been recalculated for this combustor condition.

Presented as Paper 73-1275 at the AIAA/SAE 9th Propulsion Conference, Las Vegas, Nev., November 5-7, 1973; submitted February 20, 1974; revision received June 11, 1974.

Index categories: Air-Breathing Propulsion, Subsonic and Supersonic; Thermochemistry and Chemical Kinetics; Combustion in Gases.

*Technical Area Manager, Exhaust Emissions Technology, Fuels Branch.

†Laboratory Chemical Engineer, Turbine Components Branch, presently at Mobil R&D Corp., Princeton, N.J.

‡Aerospace Engineer, Turbine Components Branch. Associate Member AIAA.

II. NO_x Model

A 1972 ASME publication by Lipfert[3] first illustrated the well-behaved nature of present aircraft gas turbine NO_x emission. A plot of NO_x emissions index, expressed in gm NO_2/kg fuel, vs combustor inlet temperature, T_3, was shown to correlate sea-level NO_x data from a wide variety of engines. Figure 1 reproduces the Lipfert correlation.

This finding has many implications for models which attempt to predict NO_x emission: 1) wide combustor aerodynamic design variations apparently retain enough similarities to yield common NO_x emission characteristics; 2) differences in fuel introduction techniques have no apparent effect on emissions from these engines; and 3) combustor inlet temperature appears to be the dominant factor. Since most compressor efficiencies are in the neighborhood of 0.85, there is a given compression ratio which corresponds to each value of T_3 (for a given ambient temperature). It is also correct,

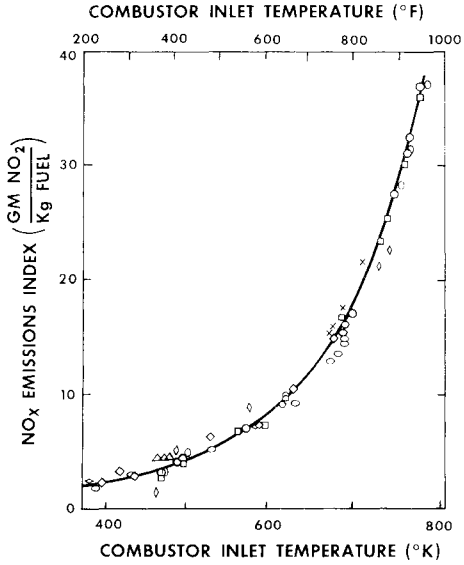

Fig. 1 NO_x emission correlation as originally presented by Lipfert in Ref.3.

therefore, to say that compressor pressure ratio is the dominant factor.

The NO_x formation model is relatively simple. Although local combustor equivalence ratios can be as high as 2.0, the important regions to consider in modeling NO_x emission are those where $\phi \approx 0.9$ because a slightly lean equivalence ratio provides the optimum combination of temperature and available oxygen radicals for the formation of NO. All results discussed in Secs. II-VII are based on $\phi = 0.9$.

Although a combination of NO and NO_2 is often detected in exhaust measurement, all results presented are based on NO formation chemistry only. Currently known NO_2 formation mechanisms involve NO as an intermediate; hence, NO kinetics yield the proper result for total NO_x emission.

Combustors used in future engines will be designed with much lower maximum equivalence ratios ($\phi \approx 0.6$). Recognizing that NO_x formation behavior may drastically change for these combustors, the important dependencies have been rederived for an assumed $\phi = 0.6$; the results are given in Sec. VIII.

The analysis includes two contributions to the NO formation process. The newly postulated "prompt NO" is the first contribution. Recent experimental results have shown the likelihood that the initial stages of combustion are dependent upon chemical kinetics of free radical formation. Radical concentrations in excess of those expected from equilibrium calculations result. Accurate analytical treatment of the free radical kinetics is tedious and uncertain, hence empirical correlations are necessary. Prompt NO can be expressed as:

$$[NO]_{prompt} = f(\phi)\, P^{1/2} [NO]_{equilibrium} \tag{1}$$

as shown by Fenimore [4] for combustion of ethylene, where [ ] denotes concentration, (g moles/cc) and P is the pressure in atm. For $\phi = 0.9$, $f(\phi) = 0.012$, and for $\phi = 0.6$, $f(\phi) = 0.006$. The results obtained for ethylene have recently been shown to be also approximately correct for such heavy hydrocarbons as gasoline.[5] By definition, $[NO]_{prompt}$ is assumed to appear instantaneously as primary zone combustion commences.

The second contribution involves NO formed through the reactions of the modified Zeldovitch mechanism which are rapid at the temperature of the primary zone. The particular reaction of importance is:

$$N_2 + O \underset{k_2}{\overset{k_1}{=}} NO + N \tag{2}$$

The importance of including both forward and reverse reactions was previously mentioned by Shaw.[6] These proceed at rates considerably greater than other reactions in the modified Zeldovitch mechanism. Consequently, Eq. (2) is the only chemical reaction considered herein.

The analysis assumes that the concentrations of O, N_2, and N correspond to their equilibrium values at the primary zone flame temperature. In the NO formation zone the rate of formation is given by the following expression:

$$d[NO]/dt = k_1 [N_2]\, [O] - k_2 [NO]\, [N] \tag{3}$$

where t = time in seconds, and the rate constants in Eq. (3) are given by[7]:

$$k_1 = 1.36 \times 10^{14} e^{-74{,}000/RT}$$

$$k_2 = 3.1 \times 10^{13} e^{-384/RT}$$

Since the temperature throughout the NO formation zone is constant and it is assumed that the concentrations of N_2, O, and N are their equilibrium values, Eq. (3) can be integrated from $t = 0$ where $[NO] = [NO]_{prompt}$ to $t = t_{res}$. Here, t_{res} represents an average time that the reactants involved in NO formation remain at a temperature corresponding to $\phi = 0.9$, rather than being a more general combustor residence time parameter. Its magnitude can be determined from available data, as shown in Sec. IV. Equation (3) then becomes:

$$[NO] = (k_1 [N_2]\, [O]/k_2 [N])[1 - \exp(-k_2 [N] t_{res})] + [NO]_{prompt} \exp(-k_2 [N] t_{res}) \tag{4}$$

The two extreme assumptions which might be employed to predict NO emission are special cases of Eq. (4). If the back reaction is extremely slow so that $k_2\,[N]t_{res}$ is a very small number and prompt NO is neglected, a Taylor series can be used to illustrate that Eq. (4) reduces to:

$$[NO] = k_1 [N_2]\, [O] t_{res} \tag{5}$$

This represents the result obtained when assuming the reaction begins with [NO] = zero and proceeds only in the forward direction. On the other hand, if t_{res} is sufficiently long or the backward reaction is fast enough, the exponential terms reduce to zero and the following equation results:

$$1 = \frac{k_1 [N_2][O]}{k_2 [N][NO]} \tag{6}$$

This is the definition of equilibrium, indicating that under these presumptions NO_x emission corresponds to the primary zone temperature equilibrium value. Actually, neither extreme is correct for the case of aircraft gas turbines, as the present model shows.

Equation 4 illustrates the strong dependence of NO_x emission on primary zone flame temperature (through k_1 and k_2), and t_{res}. The next two sections are devoted to accurate flame temperature calculation and solution for t_{res} from available data.

III. Calculation of Combustor Inlet and Flame Temperature

Examination of Eq. (4) readily illustrates that NO_x production is extremely sensitive to flame temperature. Therefore, accurate calculation of flame temperature is necessary. All factors which affect it also affect NO formation and must be included in the calculation: a) the inclusion of ambient pressure, temperature and humidity is important because of the strong observed effects on sea-level NO_x emission. The effects of altitude come about through changes in ambient temperature and pressure; b) Consideration must be given to the inlet and compressor thermodynamic processes to give accurate results for combustor inlet temperatures.

In connection with this second factor, the temperature and pressure at the compressor inlet, T_2 and P_2, must be calculated for cases where prediction of aircraft NO_x emission during high flight speed operation is required. The inlet diffuser pressure recovery is assumed to follow MIL Specification 5008B in this analysis, and the following equations are used to predict compressor inlet conditions.

$$\frac{P_2}{P_a} = \eta_r \left(\frac{T_2}{T_a}\right)^{\frac{\gamma}{\gamma - 1}} \tag{7}$$

where $\eta_r = f(M_\infty)$, γ is the ratio of specific heats, and M_∞ = flight Mach number. Further,

$$\frac{T_2}{T_a} = 1 + \frac{\gamma - 1}{2} (M_\infty)^2 \tag{8}$$

P_a and T_a are the ambient conditions.

Combustor inlet conditions may be calculated using the above results as input. The results of the compression process are calculated by knowing the compressor efficiency defined as:

$$\eta_C = \frac{\Delta h_{ideal}}{\Delta h_{actual}} = \int_{T_2}^{T_{3i}} C_p(T)\, dT \Big/ \int_{T_2}^{T_3} C_p(T)\, dT \tag{9}$$

where h = enthalpy; C_p = specific heat; T_{3i} = isentropic temperature for compression process; and T_3 = combustor inlet temperature. Equations (7)-(9) may be used to calculate the combustor inlet temperature for any pressure ratio, Mach number, and ambient temperature.

Figure 2 illustrates the effect of compressor efficiency and pressure ratio on T_3 for sea-level static conditions. For this analysis, ambient temperature, T_a, was taken to be 288K (59°F) and ambient humidity, H, was assumed to be 0 gm H_2O/gm dry air. Combustor inlet temperature is seen to increase rapidly with compressor pressure ratio. Further, note that compressor inefficiencies seriously affect temperature—at a pressure ratio of 25 and a compressor efficiency of 0.85, the deviation from the ideal is approximately 65K. For the remainder of the results discussed in this paper, a compressor efficiency of 0.85 has been assumed.

Figure 3 illustrates the variation of T_3 for changes in ambient temperatures. For example, at a pressure ratio of 30, a variation in ambient temperature from 273K (32°F) to 311K (100°F) results in an increase in T_3 of 100K. Considering the fact that reactions having high values of activation energy are very sensitive to temperature changes, this increase should certainly be expected to strongly influence NO_x emission. Note also that the slope of these curves increases slightly for increased compressor pressure ratios.

Using the relationship between T_3 and P_3 described above, the constant pressure adiabatic flame temperature may then be calculated. For this analysis, fuel was assumed to be represented by C_nH_{2n} and the enthalpies were calculated using the variable specific heat equations for all significant combustion products. The equilibrium reactions are tabulated in Table 1. The results of this analysis have been checked against established thermochemical equilibrium calculations.[8]

Of primary importance to the subject of this paper is the effect of humidity on flame temperature. Water vapor, because it increases the average specific heat, reduces flame temperature. This effect is illustrated in Fig. 4 where predicted flame temperature is plotted against combustor inlet temperature at humidities of 0, 0.01, 0.02, 0.03, and 0.05 gm H_2O/gm dry air. The consistency of the humidity effect (approximately a 21°K drop for each 0.01 gms H_2O/gm dry air of humidity regardless of inlet temperature) is noteworthy.

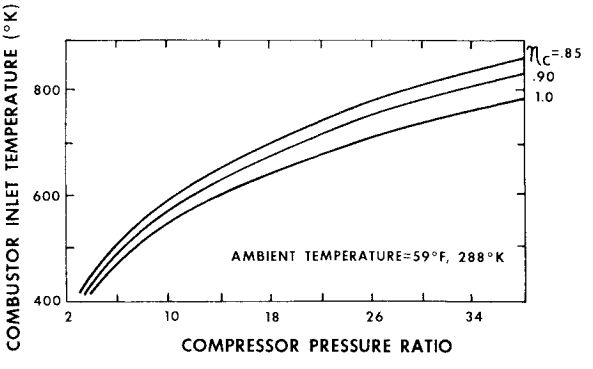

Fig. 2 Compressor pressure ratio effects on T_3.

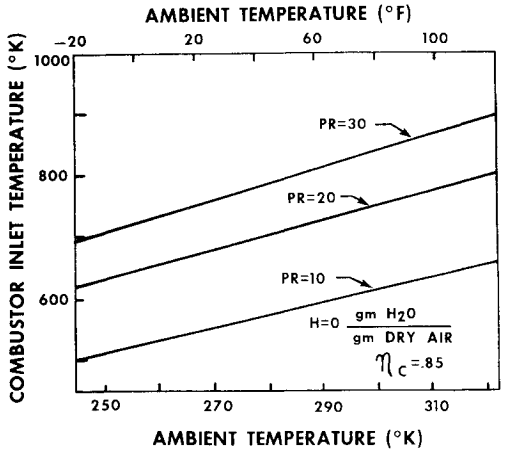

Fig. 3 Variation in T_3 with ambient temperature.

IV. Determination of t_{res} and Comparison with Data

As previously mentioned, t_{res} may be calculated from empirical data. In the present case, the Lipfert data correlation is used to give a representative condition—combustor inlet temperature of 676°K, humidity of 0.01 gm H_2O/gm dry air, and an emission index of 15. These conditions translate to sea-level static operation at 80°F (chosen to be representative of the actual conditions when these data from Ref. 9 were obtained) at a pressure ratio of 13.8 and a representative compressor efficiency of 0.85.

Equation (4) may be converted to yield emission index

Table 1 Equilibrium relations employed in flame temperature calculations[a]

1)	$H_2 + CO_2 \Leftrightarrow H_2O + CO$	$K_p = 21.7\, e^{-3286/T}$
2)	$H_2 + \frac{1}{2}O_2 \Leftrightarrow H_2O$	$K_p = 9.123 \times 10^{-4} e^{-30200/T}$
3)	$H_2 + O_2 \Leftrightarrow 2OH$	$K_p = 25.0\, e^{-8740/T}$
4)	$H_2 \Leftrightarrow 2H$	$K_p = 2.052 \times 10^{6} e^{-54,434/T}$
5)	$O_2 \Leftrightarrow 2O$	$K_p = 1.077 \times 10^{7}\, e^{-61668/T}$
6)	$N_2 \Leftrightarrow 2N$	$K_p = 3.315 \times 10^{3}\, e^{-57718/T}$
7)	$N_2 + O_2 \Leftrightarrow 2\,NO$	$K_p = 19.776\, e^{-21670/T}$

[a] Generated by curve-fitting data obtained from Ref. 12.

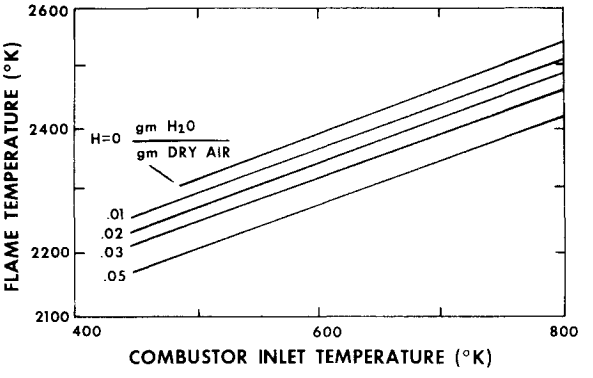

Fig. 4 Humidity effect on flame temperature.

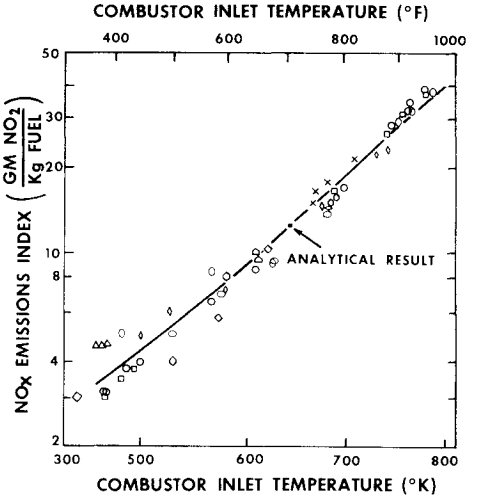

Fig. 5 Comparison of analytical result with Lipfert's data.

rather than concentration by use of the ideal gas law and knowledge of the primary zone fuel air ratio:

$$NO_xEI = 2.21 \times 10^6 (T/P)[NO] \quad (10)$$

where T = °K, P = atm, and [NO] = gm moles/cc. Inserting these conditions into Eq. (4), t_{res} is found to be approximately 0.6 msec.

Having found t_{res} for this condition, we assumed the analysis with $t_{res} = 0.6$ msec to be valid for all cases and used Eq. (4) to generate NO_x emission indices for conditions corresponding to other inlet temperatures on the Lipfert curve (while holding T_a to 80°F, humidity to 0.01 gm H_2O/gm dry air, and η_c to 0.85). Results are plotted in Fig. 5. Excellent agreement with the Lipfert data is apparent throughout the entire range of combustor inlet temperatures. This lends credibility to the previously stated assumptions (i.e., $\phi = 0.9$ and t_{res} = constant) and to the correction factors and trends to be discussed below.

The Lipfert plot for a standard day—59°F and 0 gm H_2O/gm dry air—is illustrated in Fig. 6. Two additional factors are shown: 1) the NO_x emission index which corresponds to primary zone equilibrium and 2) the amount of the NO_x which is formed as prompt NO. Note that at higher combustor inlet temperatures, the NO_x emission becomes a substantial fraction of the equilibrium amount. Clearly, at these conditions, reverse reactions must not be neglected in NO_x prediction models. The second point is that at the lower inlet temperatures the prompt NO_x contribution is predominant. This means that NO_x abatement at these conditions may be more difficult using presently proposed control techniques. This is not especially significant with regard to large high-pressure-ratio engines because these lower temperatures correspond to engine idle where NO_x is not considered to be a problem compared to emission at full power. However, auxiliary power units, which continuously operate at temperatures in this range and have been identified[1] as a significant NO_x source, will have a much more difficult problem in reducing NO_x emissions.

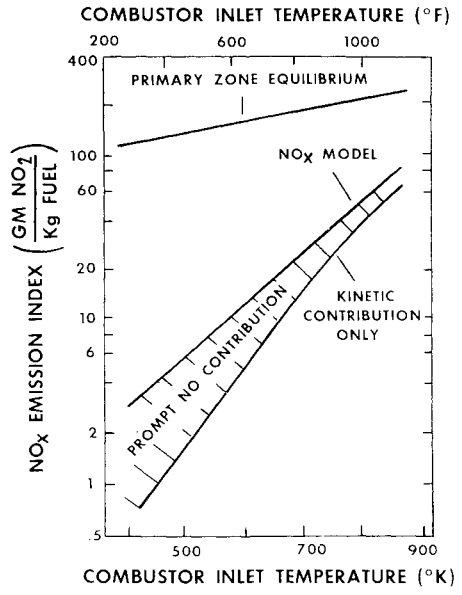

Fig. 6 Model results for standard day conditions (T_1 = 59°F, 288K; H = 0 (gm H_2O/gm dry air) illustrating primary zone equilibrium and prompt NO contribution.

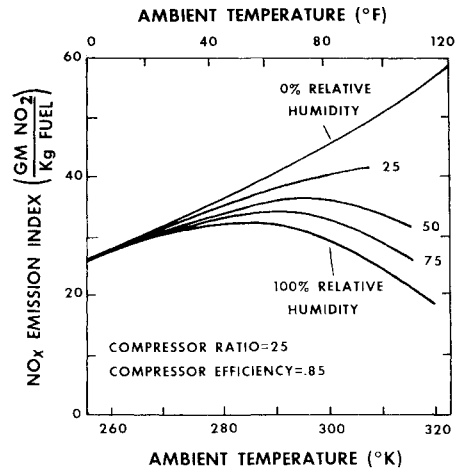

Fig. 7 Ambient condition effects on NO_x emission.

V. Corrections for Ambient Conditions

Humidity affects NO_x emission by decreasing the primary zone flame temperature as shown in Fig. 4. This decrease is due to increased C_p of the mixture with increased absolute humidity, gm H_2O/gm dry air. Naturally, for a given ambient temperature, humidity cannot be above that corresponding to saturation.

Figure 7 illustrates the predicted NO_x emission vs ambient temperature for a 25/1 compression ratio engine with a compressor efficiency of 0.85 at various inlet temperatures and humidities. The 0% humidity curve illustrates the expected

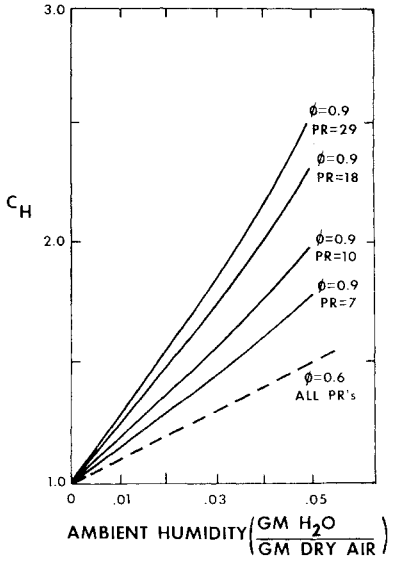

Fig. 8 Ambient humidity correction factors (ϕ = 0.9 and ϕ = 0.6).

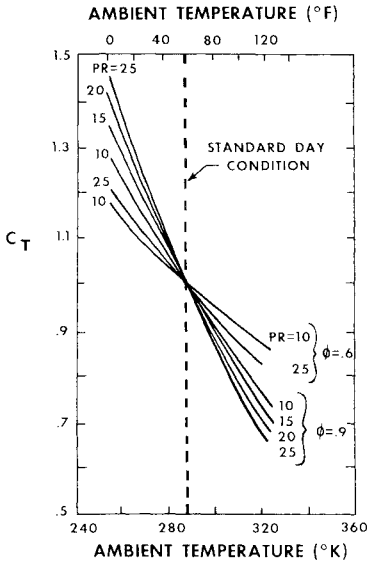

Fig. 9 Ambient temperature correction factors (ϕ = 0.9 and ϕ = 0.6).

continuous increase in NO_x with increased T_a (and therefore primary zone temperature). However, the 100% relative humidity NO_x emission actually begins to decrease with increasing ambient temperatures. The large NO_x reduction is due to the nonlinear increase in saturation absolute humidity (gm H_2O/gm dry air) at ambient temperatures above 278°K (40°F). This illustrates the importance of humidity correction at ambient temperatures above 278°K. The results of Fig. 7 agree very well with the experimental observations shown in Ref. 10. A humidity correction factor can be derived to account for these effects.

$$C_H = \frac{NO_xEI \text{ (at 0 gm } H_2O/\text{gm dry air)}}{NO_xEI \text{ (at humidity} = H)} \tag{11}$$

Use of this parameter is convenient because, when multiplied with the measured NO_x emission, the 0% humidity NO_x results.

Equation (4) has been used to calculate the value of C_H for pressures of 7, 10, 18, and 29 atm. This corresponds to T_3 values of 650, 700, 750, and 800K at sea level static. Significantly different results are obtained as the pressure ratio is changed. Lower pressure ratios have less NO_x suppression with humidity because of the large portion of the emission which is prompt NO—this contribution is less sensitive to temperature changes than the kinetically formed NO. Results are shown in Fig. 8.

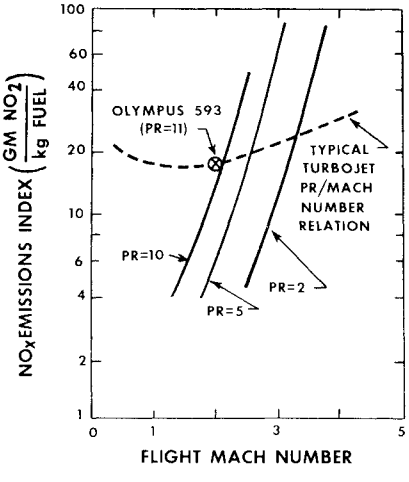

Fig. 10 NO_x emission variation with Mach number at an altitude of 60,000 ft.

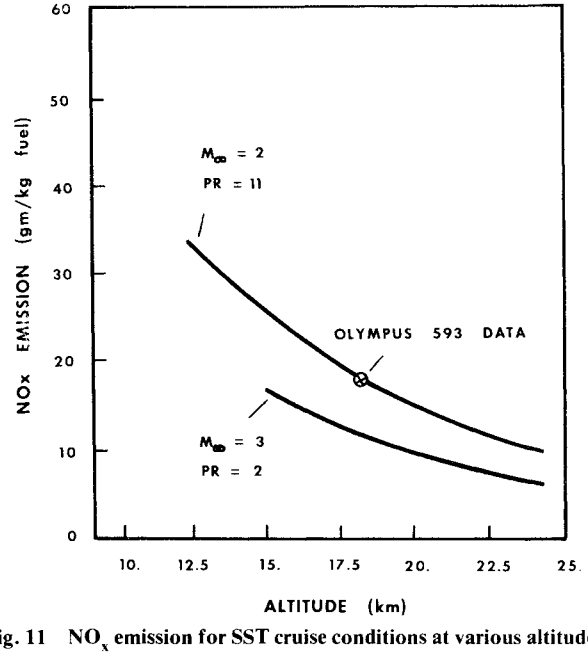

Fig. 11 NO_x emission for SST cruise conditions at various altitudes.

The model has also been used to develop correction factors for ambient temperature. In this case, corrections are made back to standard day conditions of 288K (59°F). The effect of compressor pressure ratio has been carefully studied in this analysis—combustor inlet temperature differences from those corresponding to 288K ambient temperature depend on pressure ratio as previously shown in Fig. 3. The temperature correction factor is defined as:

$$C_T = \frac{NO_xEI \text{ (288K ambient temp.)}}{NO_xEI \text{ (actual ambient temp.)}} \tag{12}$$

The results are shown in Fig. 9. Ambient temperatures from 256K to 322K (0 to 120°F) and pressure ratios between 10 and 25 have been used in the calculations. The pressure ratio effects are apparent at low ambient temperatures. Note that these correction factors were derived for ambient humidities of 0 gm H_2O/gm dry air.

VI. Stratospheric Considerations

When knowledge about NO_x emission from engines operating in flight is required, the ram temperature and pressure rise as well as compressor effects must be considered as discussed in reference to Eq. (7) and (8). Since different compressors develop different pressure ratios at a given inlet condition, and inlet conditions are a function only of flight Mach number and altitude, the T_3 and P_3 can vary widely at a given flight condition. The effect of Mach number is is particularly strong during supersonic operation; therefore; Mach number and compressor pressure ratio effects should be considered separately.

Figure 10 illustrates the effect of Mach number. Engine compressor pressure ratios of 2, 5, and 10 have been used in this calculation with compressor efficiency assumed to be 0.85. As expected, NO_x rises significantly with Mach number due to the inlet compression effect. It should be noted, however, that technology has not advanced to the point where all conditions on this plot are achievable—present material limitations preclude operation at pressure ratios much above those indicated by the dashed curve. The Olympus 593 data[11] has been plotted and is in excellent agreement with the results.

In addition to the Mach number and compressor pressure ratio effect, ambient temperature and pressure chances cause NO_x to vary. Figure 11 shows results for flight Mach numbers of 2.0 and 3.0 and compressor ratios of 11 and 2. These particular Mach numbers represent those frequently mentioned for supersonic transport operation. Decreasing NO_x emission with increasing altitude is clearly shown. Agreement of the Olympus 593 data (pressure ratio = 11 at $M_\infty = 2.0$) is again apparent.

A final matter regarding stratospheric NO_x emission involves discussion of the error incurred with use of test cell data obtained with ambient humidities of approximately 300 ppm. Because of limitations of drying capability for test cell intake air, it is difficult to supply air at humidity levels below this, yet stratospheric levels are at 3 ppm.[11] Analyses with this model indicate no cause for concern—the difference in NO_x emission between the 3 and 300 ppm levels should be less than 1/2%, as shown by Fig. 8. One ppm water = 6.22×10^{-7} gm H_2O/gm dry air.

VII. Other Applications

Two further applications for this model will be discussed here. The first is the prediction of the effectiveness of water injection into the combustor as a technique to reduce NO_x emission. Water again increases specific heat of the mixture and thus reduces flame temperature and NO_x emission. Basically, this can be modeled with the same procedure

previously used to investigate the effect of humidity. The most significant exception is that for optimum effectiveness, the water is injected into the primary zone only, and the amount is usually quantified as gm H_2O/gm fuel. For example, if half as much water as fuel is injected, this corresponds to an H of 0.03 gm H_2O/gm dry air. Figure 8 indicates that this will reduce NO_x by approximately 40% in a combustor where the pressure ratio is 29. It should be noted here that this analysis predicts the ideal effect of water injection. It is assumed that the water is evenly distributed in the primary zone, and is injected as a vapor at temperature T_3. Further NO_x supression could be gained by injecting liquid water to take advantage of the heat of vaporization.

The second application involves the determination of correction factors for combustor rig experimental results. Much data obtained with combustor rigs is obtained at the proper temperature but, because of facility limitations, at pressures reduced from the design value. NO_x emission data obtained is usually corrected by multiplying the square root of the ratio of the design pressure to the combustor rig pressure, $P_d/P_c^{1/2}$. A rationale for this correction factor is found by manipulation of Eq. (5) with the assumption that the flame temperature does not vary with pressure.

Because of the errors inherent in Eq. (5) and the fact that flame temperature decreases with decreasing pressure, an improved correction factor has been calculated using Eq. (4). Results are shown in Fig. 12. The departure from $(P_c/P_c)^{1/2}$ is significant, especially at P_d/P_c values above 4.0.

VIII. Low Emissions Combustors

Since combustors designed for low NO_x emission will probably have a maximum primary zone equivalence ratio of 0.6, the C_H, C_T and pressure ratio correction factors derived above are not applicable. Using identical procedures, new values have been calculated for $\phi = 0.6$. Because no significant differences in combustor length or reference velocities are anticipated, t_{res} was assumed to remain 0.6 msec. The analysis predicts values of NO_x emissions index in the range of 7-10, depending on pressure ratio, for the $\phi = 0.6$ design. This agrees well with the contract goal established by NASA in their present Clean Combustor Program.

The new C_H and C_T values are illustrated in Figs. 8 and 9. Weaker influences of H and T_a are a result of lower operating temperature. The rederived pressure correction factors in Fig. 12 are in excellent agreement with the $(P_d/P_c)^{1/2}$ dependence because, as temperature is decreased less CO and H_2 are present as equilibrium to reduce flame temperature.

IX. Summary and Conclusions

A relatively simple model has been used to predict aircraft turbine engine NO_x emissions. Prompt NO and the predominant NO formation and destruction reactions are considered in the analysis. Key assumptions include constant NO formation time, primary zone equivalence ratio of 0.9 and equilibrium concentrations of N_2, N, and O.

Correction factors for ambient humidity and temperature have been derived from the model. These factors correct data obtained at given ambient conditions to standard day conditions—288K (59°F) and zero gm H_2O/gm dry air humidity.

Questions in connection with stratospheric NO_x emission are addressed. Mach number is shown to strongly influence NO_x emission due to the ram effect on temperature and pressure. Altitude is shown to reduce NO_x emission because of reduce ambient pressure and temperature. The ideal effectiveness of combustor water injection for NO_x abatement is evaluated. Analyses show that significant reductions can be achieved.

Correction factors for NO_x data obtained in combustor rigs operating at pressures below the design value are derived. It is found that the previously used pressure correction factor $(P_d/P_c)^{1/2}$ can significantly underpredict the necessary correction for combustors where the primary zone equivalence ratio conforms to the $\phi = 0.9$ assumption. This results because of decreased flame temperature as pressure is decreased—a factor not included in the analysis resulting in $(P_d/P_c)^{1/2}$.

Other conclusions are: 1) primary zone residence time for NO formation is approximately constant for a wide variety of present engines; 2) prompt NO is a significant contributor to NO_x emission at low inlet temperature. This indicates that NO_x control at conditions where APU's continuously operate may be more difficult than previously expected; 3) NO_x levels at high combustor inlet temperatures (850K) begin to approach equilibrium levels at $\phi = 0.9$. Models to predict NO_x emission in future high compression engines should not neglect the reverse reaction. Because future combustors will operate near $\phi = 0.6$ in the primary zone, the pertinent dependencies have been recalculated for these conditions. Weaker dependencies on ambient humidity and temperature and a pressure correction factor close to $(P_d/P_c)^{1/2}$ are apparent.

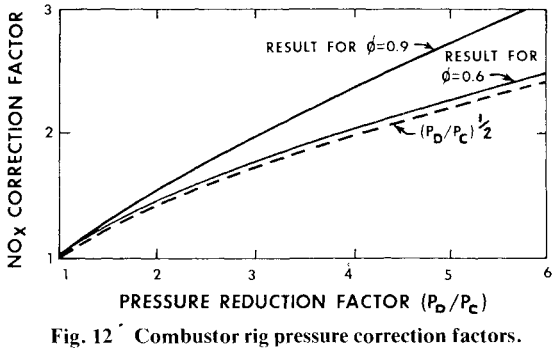

Fig. 12 Combustor rig pressure correction factors.

References

[1]U.S. Environmental Protection Agency, "Control of Air Pollution from Aircraft and Aircraft Engines," *Federal Register,* Vol. 38, No. 136. July 17, 1973.

[2]Society of Automotive Engineers Committee E-31, "Procedure for the Continuous Sampling and Measurement of Gaseous Emissions from Aircraft Turbine Engines," SAE Aerospace Recommended Practice 1256, Oct. 1971.

[3]Lipfert, F. W., "Correlation of Gas Turbine Emissions Data," ASME Paper 72-GT-60, March 1972.

[4]Fenimore, C. P., "Formation of Nitric Oxide in Premixed Hydrocarbon Flames," *13th Symposium (International) on Combustion,* 1970.

[5]Bachmaier, F., Eberius, K. H., and Just, T. H., "The Formation of Nitric Oxide and the Detection of HCN in Premixed Hydrocarbon-Air Flames at 1 Atmosphere," *Combustion Science and Technology,* Vol. 7, 1973, pp. 77-84.

[6]Shaw, H., "Fuel Modification for Abatement of Aircraft Turbine Engine Oxides of Nitrogen Emissions," AFAPL-TR-72-80, Oct. 1972, (AD-742,581), Air Force Aero Propulsion Lab. Wright-Patterson Air Force Base, Ohio.

[7]Bauch, D. L., Drysdale, D. D., Horne, D. G., and Lloyd, A. C., "Critical Evaluation of Rate Data for Homogeneous, Gas Phase Reactions of Interest in High Temperature Systems," No. 4, Dec. 1969, Dept. of Physical Chemistry, The University Leeds, Leeds, England.

[8]Fremont, H. A., Powell, H. N., Shaffer, A., and Sucia, S. N., *Properties of Combustion Gases,* Vol. I and II, Aircraft Gas Turbine Development Dept., General Electric Co., Cincinnati, Ohio, 1955.

[9]Bogdan, L. and McAdams, H. T., "Analysis of Aircraft Exhaust Emissions Measurement," Rept. NA-5007-K-1, Oct. 1971, Cornell Aeronautical Lab, Buffalo, N.Y.

[10]Nelson, A. W., "Detailed Exhaust Emissions Measurements of Three Different Turbofan Engine Designs," *Atmospheric Pollution by Aircraft Engines,* AGARD Conference Proceedings, No. 125, April 1973.

[11]Williams, M. R., "Emission Levels of the Olympus 593 Engine at Stratospheric Cruise Conditions of the Concorde Aircraft," *Proceedings of the Second CIAP Conference, Nov. 1972,* edited by Broderick, A. J., Dept. of Transportation, TSC-OST-73-4, Department of Transportation, Washington, D.C.

[12]JANAF Thermochemical Tables, revised to June 30, 1963, The Dow Chemical Co., Midland, Mich.